

*Assembly & Characterization of
Peptide Conjugated PEG-PCL Micelles*



6.1 MATERIALS

1-ethyl-3-[3-dimethylaminopropyl] carbodiimide (EDC) and dialysis tube (MWCO 12000) were purchased from Sigma Aldrich, Mumbai. *N*-hydroxysuccinimide (NHS) and trehalose were bought from Himedia Lab, Mumbai. Pentapeptide, YIGSR-NH₂ (Tyr-Ile-Gly-Ser-Arg-NH₂) and EILDV-NH₂ (Glu-Ile-Leu-Asp-Val-NH₂) were procured from Bioconcept Lab. Pvt. Ltd., Haryana and National Institute of Research in Reproductive Health [NIRRH], Mumbai respectively. Disodium hydrogen phosphate (Na₂HPO₄), potassium dihydrogen phosphate (KH₂PO₄), sodium chloride (NaCl) and sucrose were purchased from S. D. Fine-chem. Ltd., Mumbai. Poloxamer-188 was purchased from BASF, Mumbai.

6.2 ASSEMBLY OF PEPTIDE CONJUGATED MICELLES

Peptide YIGSR-NH₂/ EILDV-NH₂ was conjugated to carboxyl group present on the surface of PEG-PCL micelles using NHS and EDC as reaction promoters using method reported earlier with slight modification (Farokhzad et al., 2004; Lopez et al., 2004).

Functionalized PEG-PCL micelles were prepared by similar way using a blend of synthesized copolymer BCP and FBCP as described in chapter 4.2. Briefly, 40 mg of BCP 2-3.5 and 4.45 mg of FBCP 2-3.5 or 40 mg of BCP 5-7 and 4.45 mg of FBCP 5-7 were dissolved in acetone (3 or 4 ml) along with 2 mg of ETO and injected dropwise to 5 ml of distilled water under stirring and stirring was continued till complete evaporation of acetone. Residual amount of acetone was removed by rotary vacuum evaporator. To this, EDC and NHS dissolved in phosphate buffer pH 4.5 were added at molar concentration 4 fold excess to FBCP polymer and pH adjusted to 5.5 with 0.1 N NaOH. The resulting micellar solution was stirred at room temperature for 15 min to activate carboxyl group followed by adjusting the pH to 7.5 using 0.1 N NaOH. Desired quantity of peptide YIGSR-NH₂ or EILDV-NH₂ dissolved in PBS pH 7.4 was added (HOOC-PEG-PCL: peptide, 1:1 molar ratio) to micellar solution and incubated for 3 h under mild stirring at room temperature. After conjugation, micellar solution was dialyzed using dialysis tube (MWCO 12000) for 1 h against distilled water to remove unconjugated peptide and by products formed during amide bond formation. Finally, micellar solution was filtered through 0.45 micron membrane filter.

The amount of peptide bound to micelles was determined by developed TNBS assay method (Chapter 3.3), measuring unconjugated peptide found in dialysis medium. Conjugation efficiency of peptide to micelles was assessed by varying various parameters i.e. incubation temperature and time as well as molar ratio of peptide to functional polymer. Optimized batch was assessed for particle size, zeta potential and percent drug entrapment before and after conjugation of peptide. YIGSR conjugated PEG-PCL micelles of definite molecular weight were denoted as YPCL235 and YPCL570 while EILDV conjugated micelles were denoted as EPCL235 and EPCL570.

6.3 CHARACTERIZATION OF MICELLAR FORMULATION

6.3.1 Differential scanning calorimetry

DSC thermograms of ETO, MPCL235 and MPCL570 were acquired by use of DSC60-A differential scanning calorimeter (Shimadzu, Japan) to find out physical state of formulation after encapsulation. About 2.5 mg of samples were crimped in standard aluminum pans with lids and the sample was purged with pure dry nitrogen at flow rate of 30 ml/min. The temperature ramp speed was set at 10 °C/min with heat flow rate between room temperature to 300 °C. Indium was used as the internal standard reference material to calibrate the temperature and energy scales of the DSC instrument.

6.3.2 X-ray diffractogram

X-RD of ETO and lyophilized MPCL235, MPCL570 was performed using Bruker AXS D8 Advance X-ray diffractometer with DIFFRAC plus software (version 3.2) (Bruker Inc., Madison, WI) using Cu-K α radiation. Approximately 30 mg pure drug or lyophilized samples MPCL micelles was placed on a zero background quartz plate and continuously scanned at a rate of 0.75° 2 θ /min over a range of 5° to 50° 2 θ .

6.3.3 Transmission electron microscopy

The morphological examination of MPCL235 and MPCL570 micelles were performed using Philips Technai-20. 200 KV, transmission electron microscope after negative staining with 1 % uranyl acetate. Micellar formulations were placed and dried on carbon coated copper grid. Negative staining was performed using drop of

1 % uranyl acetate solution and kept for 15 min at room temperature and observed under TEM.

6.3.4 Lyophilization

Lyophilization (freeze drying) technique is one of the most suitable methods to make it possible to satisfy the requisite of long-term product stability. Lyophilization of formulations was performed using cryoprotectant sucrose and trehalose at different weight ratio to the total solid content of formulation. Poloxamer-188 was also used at different ratio along with sucrose to check the redispersibility of lyophilized formulation. Briefly, definite amount of cryoprotectant with or without poloxamer-188 was dissolved to micellar solution and frozen at -40 °C. Samples were then lyophilized for 24 h using Heato Dry Winner (Germany) under vacuum. The resulting lyophilized products were sealed immediately and stored at 2-8 °C. After lyophilization, samples were reconstituted with distilled water and vortexed for 3 min to uniformly redisperse the solid content. Particle size of samples was analyzed using Zetasizer, Nano-ZS (Malvern Inst., U.K.).

6.3.5 *In vitro* release studies

In vitro release studies of ETO loaded formulation was carried out using dialysis bag diffusion technique as reported earlier (Zhang et al., 2004; Lin et al., 2005). Prior to use, the dialysis tube (MWCO 12000) was activated using procedure mentioned by manufacturer (Sigma Aldrich, Mumbai) to remove contaminants, such as glycerin and sulfur compounds. The micellar dispersion equivalent to 1 mg of ETO was filled in cellulose dialysis tube and sealed at both ends. The bag containing formulation was then dipped in container having 50 ml of PBS pH 7.4, stirred at 50 ± 5 rpm and maintained at 37 ± 2 °C. Samples were withdrawn at specified time points and the release medium was replaced by the same volume of fresh medium. The release of drug was quantified by UV-visible spectrophotometer (UV 1700, PharmaSpec, Shimadzu, Japan) at wavelength of 284 nm. The cumulative amount of drug released at each sampling point was corrected with the volume of the release medium and a graph of percent cumulative release vs. time was plotted.

6.3.6 Stability studies

Short term stability studies of lyophilized formulation were carried out at 2-8 °C (refrigerator) and at 25 ± 2 °C with 60 ± 5 % RH. At regular time interval samples were withdrawn and reconstituted with distilled water. Particles size and percent drug loading were estimated and evaluated with respect to storage condition.

6.4 RESULTS AND DISCUSSION

6.4.1. Assembly of peptide conjugated micelles

Conjugation of peptide YIGSR-NH₂ or EILDV-NH₂ to carboxyl functionalized PEG-PCL micelles was carried out using NHS and EDC through amide bond linkage. EDC is a dehydrating agent used to activate carboxylate groups to reactive o-acylisourea (Staros et al., 1986) but the formed group is unstable and short-lived in aqueous solution. It is because of the hydrolysis of o-acylisourea, regenerating the initial carboxyl group and hence it is necessary to add NHS, which reacts with the o-acylisourea to yield a semi-stable amine reactive NHS-ester with half-life of 4-5 h at pH 7.0 (Grabarek et al., 1990). The final reaction with amines is greatly favored with a stable amine bond formation. This method permits two-step crosslinking procedures, which allows the carboxyl groups eventually present on molecule to remain unaltered. This method has an advantage that it maintains intrinsic properties of ligand attached. The conjugation of ligand to the functional group of polymer can be achieved by two different means i.e. pre-insertion method and post-insertion method. In pre-insertion method, ligand is conjugated to functional polymer before formation of micelles, while in post-insertion method, micelles is assembled first and ligand is attached afterwards which ensures that ligand is attached to chemically available sites on the surface of micelles (Sutton et al., 2007). A c-RGD attached PLA-PEG micelles loaded with doxorubicin was reported with conjugation of ligand by both pre and post-insertion method (Sutton et al., 2007). They observed that c-RGD attachment to already formed micelles resulted in marked increase in cell uptake compared to ligand attachment before assembly. Although, these two methods would look to be similar, the difference is observed in the consideration of polydisperse nature of PEG chain part. In pre-insertion method, ligands are likely to conjugate the shorter PEG chain within the population and suffer from shielding effect, while in later method ligand would attach to the longer PEG chain which is extended out the surface of micelles (Sutton et al., 2007).

It is essential to have an optimal peptide density on the surface of micelles. The optimal density was defined as number of molecules of peptide on the surface of nanoparticle/ micelles to confer maximum targeted cellular uptake with avoidance of unnecessary masking of PEG on nanoparticle/micelles by excess peptide that will not give additional targeting benefit (Gu et al., 2008). Adjusting the density of peptide on the surface, the antibiofouling properties of PEG can be retained which is required for its long circulation. Moreover, Zhao & Yung (2008) reported folate conjugated PLGA-PEG micelles with different surface folate content and observed that it is required to have an optimum number of folate molecules. They also stated that too many numbers of folate molecules on the surface of micelles may result in binding of single micelles to multiple receptors leads to decrease in cellular uptake. It is also reported that high amount of intracellular folate, in the range of 2×10^7 to 9×10^7 folate molecules per cell may lead to saturation and shut off of the folate receptor (Leamon & Low, 1991; Lee & Low, 1994). However in case of peptides, it is very difficult to define the actual surface density required on the surface of micelles for maximum cellular uptake. Moreover, cellular uptake may depend on the various aspects like nature of ligand and receptor, the extent of over expression of receptor, size of nanocarrier etc. In this experiment, peptide conjugation was optimized with peptide density of 10 % using a blend of functional polymer (FBCP) and non functional polymer (BCP). Micellar formulations with surface density of 5 and 20 percent were also prepared after optimization of process and formulation parameters to assess the maximum cellular uptake of micelles.

A post-insertion method consisting of two step reaction was performed to form amide bond between free terminal amine group of peptide (YIGSR-NH₂ and EILDV-NH₂) and carboxyl group present on surface of PEG-PCL micelles. The conjugation efficiency of peptide YIGSR-NH₂ and EILDV-NH₂ was assessed by changing various parameters like incubation temperature, incubation time and ratio of functional polymer (FBCP) to peptide. The molar concentration of EDC and NHS used was 4 times higher to that of functional polymer used. After conjugation, the micellar solution was dialyzed against distilled water and the unconjugated peptide found in dialyzed medium was estimated by developed TNBS method (Chapter 3.3).

Initially, reaction or incubation temperature was optimized carrying out the incubation of peptide with micelles formulation at room temperature and at 4 °C for 3 h. As shown in Table 6.1, there was no any significant difference found in percent conjugation at both the conditions. The percent conjugation of YIGSR-NH₂ in YPCL235 and YPCL570 at room temperature was found 87.98 ± 4.70 and 88.30 ± 5.19 respectively while at 4 °C it was observed 86.65 ± 6.33 & 85.29 ± 3.08 respectively. Similarly, the percent conjugation of EILDV-NH₂ in EPCL235 and EPCL570 at room temperature was found 85.34 ± 7.42 & 89.26 ± 6.30 respectively while at 4 °C; it was 86.01 ± 6.94 & 90.50 ± 4.23 percent. The results obtained showed that conjugation efficiency of peptide did not affect by the incubation temperature and hence further experiments were conducted with incubation at room temperature.

Incubation condition	% Conjugation of YIGSR-NH ₂		% Conjugation of EILDV-NH ₂	
	YPCL235	YPCL570	EPCL235	EPCL570
Room temp	87.98 ± 4.70	88.30 ± 5.19	85.34 ± 7.42	89.26 ± 6.30
4 °C	86.65 ± 6.33	85.29 ± 3.08	86.01 ± 6.94	90.50 ± 4.23

Table 6.1 Effect of incubation condition on percent conjugation of peptide (Results are mean ± S. D. and n=3)

Secondly, effect of incubation time on percent conjugation was evaluated at three different time point i.e. 1 h, 3 h and 6 h. At 1 h incubation, the percent conjugation of both the peptide was found between 39.34 to 51.12 percent (Table 6.2). Incubation time of 3 h, showed conjugation of YIGSR-NH₂ to 87.98 ± 4.70 and 88.30 ± 5.19 percent for YPCL235 and YPCL570 respectively. EILDV-NH₂ conjugated micelles EPCL235 and EPCL570 showed 85.34 ± 7.42 & 89.26 ± 6.30 percent conjugations respectively at 3 h of incubation. A further increase in incubation time upto 6 h showed no any improvement in conjugation of peptide in all the formulations, which might be due to saturation and variation in chain length of HOOC- PEG-PCL chains.

Time of incubation	% Conjugation of YISGR-NH ₂		% Conjugation of EILDV-NH ₂	
	YPCL235	YPCL570	EPCL235	EPCL570
1 h	45.07 ± 7.83	51.12 ± 3.56	39.34 ± 3.01	46.41 ± 3.98
3 h	87.98 ± 4.70	88.30 ± 5.19	85.34 ± 7.42	89.26 ± 6.30
6 h	89.90 ± 5.12	90.76 ± 4.57	84.09 ± 5.20	89.34 ± 4.23

Table 6.2 Effect of time of incubation on percent conjugation of peptide (Results are mean ± S. D. and n=3)

The important parameter for conjugation of peptide is the molar ratio of peptide to that of functional polymer present in micelles. The molar ratio of functional polymer to peptide was kept at three different level i.e. 1.0:0.75, 1.0:1.0 and 1.0: 1.25. At molar ratio of 1.0:0.75, the percent conjugation of peptide YIGSR-NH₂ in YPCL235 and YPCL570 was found 67.55 ± 3.87 & 71.82 ± 7.09 respectively (Table 6.3) while at the same ratio, conjugation of EILDV-NH₂ was found 68.32 ± 5.80 & 63.53 ± 6.01 percent for EPCL235 and EPCL570 respectively. It was observed that at 1.0:1.0 molar ratio, maximum conjugation of peptide took place. A further increase in the molar ratio resulted in to no any significant increase in peptide conjugation (Table 6.3), which indicated that 1.0:1.0 ratio of functional polymer to peptide was sufficient for maximum conjugation. Lopez et al. (2004) also reported that at 1.0:1.0 ratio of DSPE-PEG-COOH to peptide, maximum conjugation upto 80 % was achieved.

FBCP: peptide (molar ratio)	% Conjugation YIGSR-NH ₂		% Conjugation of EILDV-NH ₂	
	YPCL235	YPCL570	EPCL235	EPCL570
1.0: 0.75	67.55 ± 3.87	71.82 ± 7.09	68.32 ± 5.80	63.53 ± 6.01
1.0:1.0	87.98 ± 4.70	88.30 ± 5.19	85.34 ± 7.42	89.26 ± 6.30
1.0:1.25	87.04 ± 5.12	87.99 ± 3.76	86.81 ± 5.55	86.56 ± 4.31

Table 6.3 Effect of ratio of functional polymer to peptide on percent conjugation of peptide (Results are mean ± S. D. and n=3)

Formulation code	Particle size (nm)		Zeta Potential (mV) at pH 7.5		PDE	
	Before	After	Before	After	Before	After
YPCL235	36.95 ± 2.34	45.23 ± 3.77	-20.9 ± 3.44	-5.74 ± 1.33	83.32 ± 2.03	77.81 ± 4.29
YPCL570	73.21 ± 4.09	83.80 ± 4.22	-21.3 ± 3.03	-5.16 ± 2.01	91.06 ± 3.48	85.50 ± 3.70
EPCL235	37.31 ± 3.22	46.20 ± 4.51	-22.6 ± 2.88	-6.79 ± 1.99	81.98 ± 4.00	75.35 ± 3.66
EPCL570	72.57 ± 3.90	80.32 ± 4.89	-19.8 ± 3.19	-5.39 ± 2.24	90.70 ± 4.81	83.98 ± 4.90

Table 6.4 Effect of peptide conjugation on particle size, zeta potential and percent drug entrapment (Results are mean ± S. D. and n=3)

Optimized batch of peptide conjugated micelles were evaluated for particle size, zeta potential and percent drug entrapment before and after peptide conjugation. It was observed as shown in Table 6.4 that, particle size increased upto 10 nm in all formulation after conjugation, which showed the evidence of peptide conjugation. Moreover, a decrease in zeta potential after conjugation was also observed at pH 7.5, which indicates the surface free carboxyl groups on micelles were utilized for formation of amide bond to amine groups of peptide. A reduction in percent drug entrapment upto 6 percent was also observed, which might be due to initial burst release of drug occurred during incubation and removed from micelles in dialysis step.

6.4.2 Characterization of micelles

6.4.2.1 Differential scanning calorimetry

DSC thermograms of samples were carried out to investigate the physical state of the drug in the micelles, because this aspect could influence the *in vitro* and *in vivo* release of the drug from the system. The drug content of micelles may be amorphous or crystalline. Moreover, a drug may be present either as dissolved or as a solid dispersion in the micelles (Atyabi et al., 2009). The DSC thermograms of pure ETO and lyophilized samples of MPCL235 and MPCL570 micelles are shown in Figure 6.1.

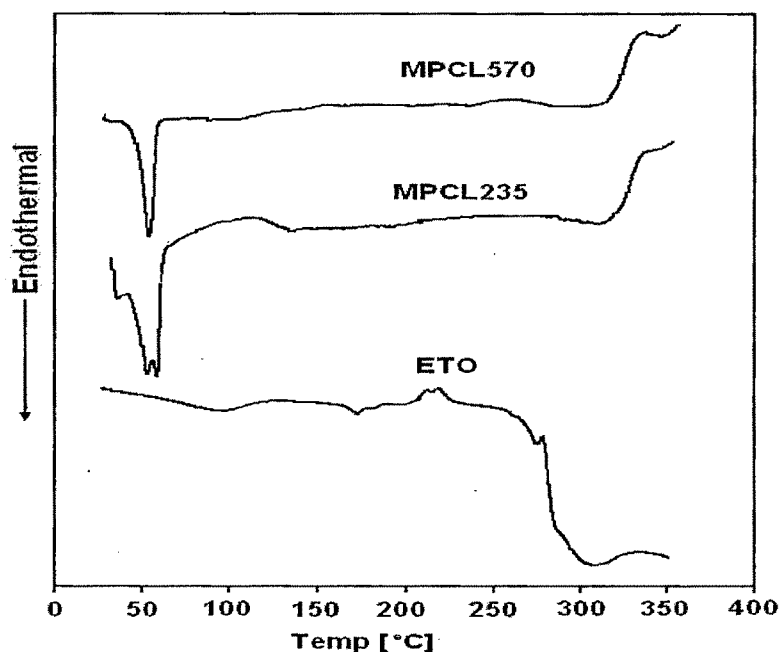


Figure 6.1 Differential scanning calorimetry thermograms of pure ETO and ETO loaded MPCL235 and MPCL570 micelles

The pure ETO showed an exothermic peak near to 210 °C and endothermic peak at 172.8 and 276 °C, which was absent in thermograms of ETO loaded MPCL235 and MPCL570 micelles (Figure 6.1). DSC thermograph of MPCL235 and MPCL570 showed an endothermic peak near to 60 °C was attributed to melting of PEG and PCL blocks (Forrest et al., 2006a). The results showed that, the encapsulated drug did not interact with the polymers and found encapsulated in the micelles. Further, results obtained were in agreement with previously reported findings (Snehalatha et al., 2008). Therefore, it could be concluded that ETO in the micelles was in molecular dispersion state or a solid solution state in the polymer matrix after micelles formation (Atyabi et al., 2009).

6.4.2.2 X-ray diffraction

The crystallization behavior of an amphiphilic copolymer greatly influences the biodegradation performance of the formed nanoparticles (Yang et al., 2007). Figure 6.2 shows the X-ray diffraction pattern of pure ETO, MPCL235 and MPCL570 micelles. ETO showed its characteristic peaks at 2θ values of 13.3°, 17.3°, 19.4°, 22.3°, 26.9°, 31.2° and 33.6° (Figure 6.2) and was similar to previously reported data (Jasti et al., 1995).

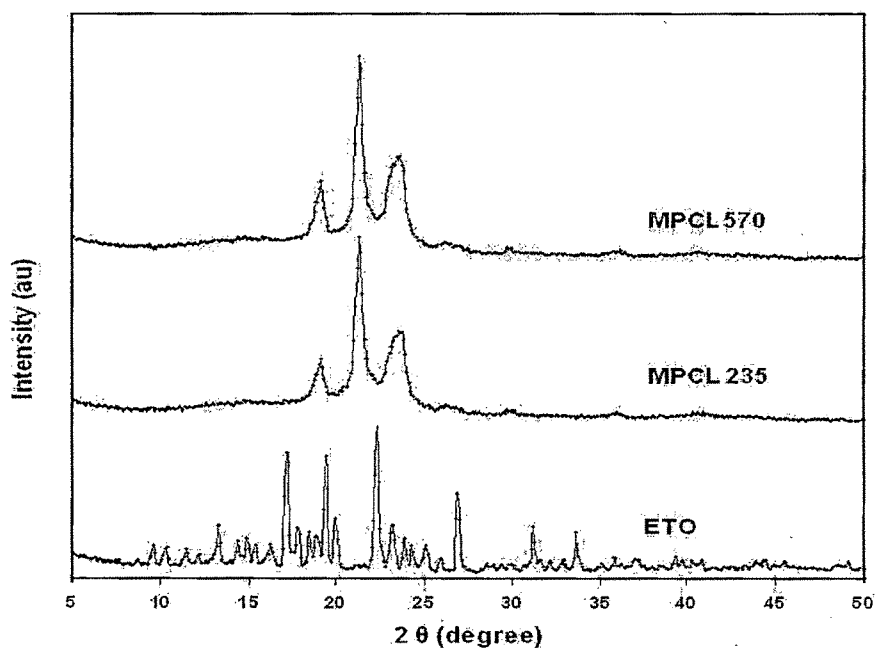


Figure 6.2 Powder X-ray diffraction patterns of ETO and ETO loaded MPCL235 and MPCL570 micelles

It was observed that after lyophilization both MPCL235 and MPCL570 were crystalline with sharp peaks at 2θ angle of 19.1 and 21.3 corresponding to PEG and PCL blocks, respectively (Figure 6.2). A third broad peak at 23.7 in MPCL235 and MPCL570 was due to overlap of secondary PEG and PCL peaks. The results obtained were in concurrence with studies carried out by Forrest et al (2006b) with PEG-PCL micelles containing rapamycin. Further, a peak at 2θ value at 19.1 and 23.7 indicating evidence of phase separation in the solid block (Zhang et al., 1996).

The release profile of drug delivery system depends upon the state of incorporated drug in nanoparticles (Zhang et al., 2004) and hence, it is important to know the state of the incorporated drug in micelles. Comparing the X-ray diffraction peaks of ETO with MPCL235 and MPCL570, it was observed that peaks of ETO disappeared in ETO loaded micelles MPCL235 and MPCL570 (Figure 6.2). It was deduced that ETO was either molecularly dispersed or distributed in an amorphous state in the PCL core (Zhang et al., 1996; Forrest et al., 2006b).

6.4.2.3 Transmission electron microscopy

Transmission electron microscopy images (Figure 6.3 & 6.4) of MPCL235 and MPCL570 revealed that micelles are of spherical shape. The diameters of micelles observed were in good agreement with the determination of particle size by DLS method.

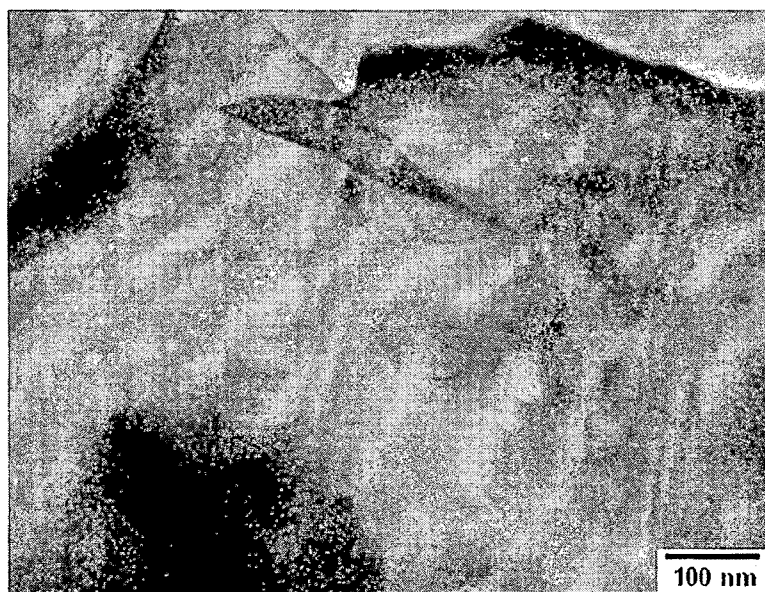


Figure 6.3 TEM images of MPCL235 micelles after negative staining with 1% uranyl acetate

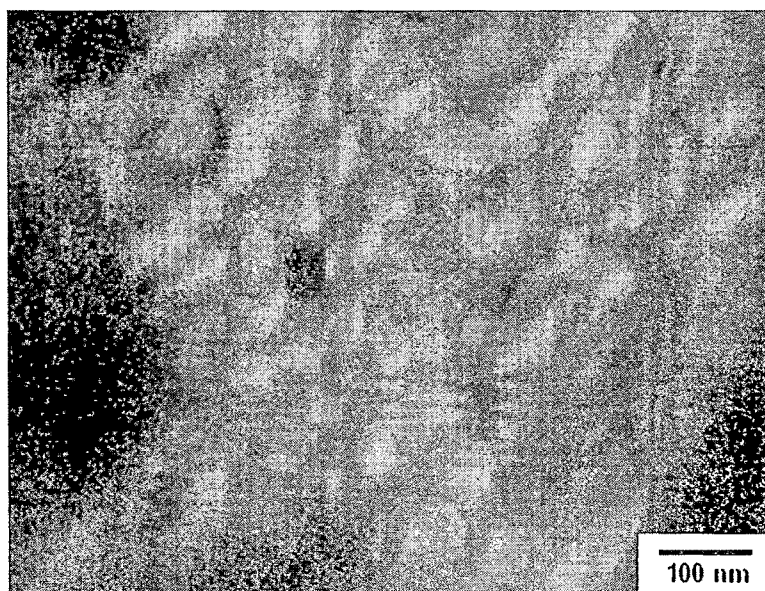


Figure 6.4 TEM images of MPCL570 micelles after negative staining with 1% uranyl acetate

6.4.2.4 Lyophilization study

To improve the long term stability of colloidal nanoparticles/ micelles, lyophilization has considered as a suitable technique (Abdelwahed et al., 2006). Generally, nanoparticles show poor long-term stability due to different physical and chemical factors that may destabilize the system. Nevertheless, a real barrier against the clinical use of nanoparticles is due to its physical instability (aggregation/particle fusion) and/or to the chemical instability (hydrolysis of polymeric materials forming the nanoparticles, drug leakage of nanoparticles and chemical reactivity of drug during the storage) which are frequently noticed when these nanoparticles aqueous suspensions are stored for an extended periods (Auvillain et al., 1989; Chacon et al., 1999).

A freeze dried nanoparticles should have certain desirable characteristics like preservation of primary physical and chemical properties of the product and should have short reconstitution time with unmodified particle size and its distribution (Abdelwahed et al., 2006). In order to protect the product from freezing stress, to maintain their properties and initial particle size, cryoprotectants are added during freeze drying. The most popular cryoprotectants used for freeze-drying of nanoparticles are sugars like trehalose, sucrose, glucose and mannitol. A suggested stabilization mechanism of nanoparticles by cryoprotectants during drying steps is the water replacement hypothesis which has explained by Allison et al. (1996 & 1998). This mechanism supposes the formation of hydrogen bonds between a cryoprotectant and the polar groups on the surface of nanoparticles at the end of the drying process. Hence, cryoprotectants preserve the native structures of nanoparticles by serving as water substitutes.

Lyophilization of micellar formulations was carried out using cryoprotectant sucrose and trehalose which was reported to have good cryoprotectant properties (Saez et al., 2000). Initially, lyophilization was carried out using sucrose or trehalose in the weight ratio of total solid content to cryoprotectant of 1:1, 1:3, 1:5, 1:7 & 1:10. Lyophilized formulations were reconstituted with distilled water and vortexed well to redisperse the suspension followed by particle size measurement. The redispersibility index was calculated based on the ratio of particle size obtained after reconstitution to that of original or initial particle size. Table 6.5 & 6.6 and Figure 6.5 & 6.6 shows the

effect different amount of cryoprotectant (sucrose or trehalose) on particle size of micelles after reconstitution i.e. redispersibility index.

Ratio*	Redispersibility index (RI) ± S.D.					
	MPCL235	YPCL235	EPCL235	MPCL570	YPCL570	EPCL570
Initial Particle Size (nm)	39.83 ± 2.53	43.23 ± 3.45	47.78 ± 3.98	71.98 ± 4.38	83.59 ± 3.08	82.32 ± 5.09
1:1	7.82 ± 0.64	8.76 ± 0.86	8.33 ± 0.62	8.19 ± 0.81	6.89 ± 0.93	7.33 ± 0.73
1:3	6.31 ± 0.85	7.17 ± 0.94	6.74 ± 0.50	5.46 ± 0.73	5.25 ± 0.66	6.09 ± 0.54
1:5	5.15 ± 0.58	6.56 ± 0.61	5.34 ± 0.49	4.70 ± 0.49	4.44 ± 0.47	4.72 ± 0.64
1:7	4.61 ± 0.74	4.15 ± 0.39	3.78 ± 0.46	3.44 ± 0.44	3.06 ± 0.35	3.65 ± 0.42
1:10	3.44 ± 0.75	3.33 ± 0.58	3.06 ± 0.53	1.91 ± 0.55	1.93 ± 0.63	2.16 ± 0.29

* Weight ratio of total solid content to sucrose

Table 6.5 Redispersibility index of micellar formulations at various weight ratios of total solid content to sucrose (n=3)

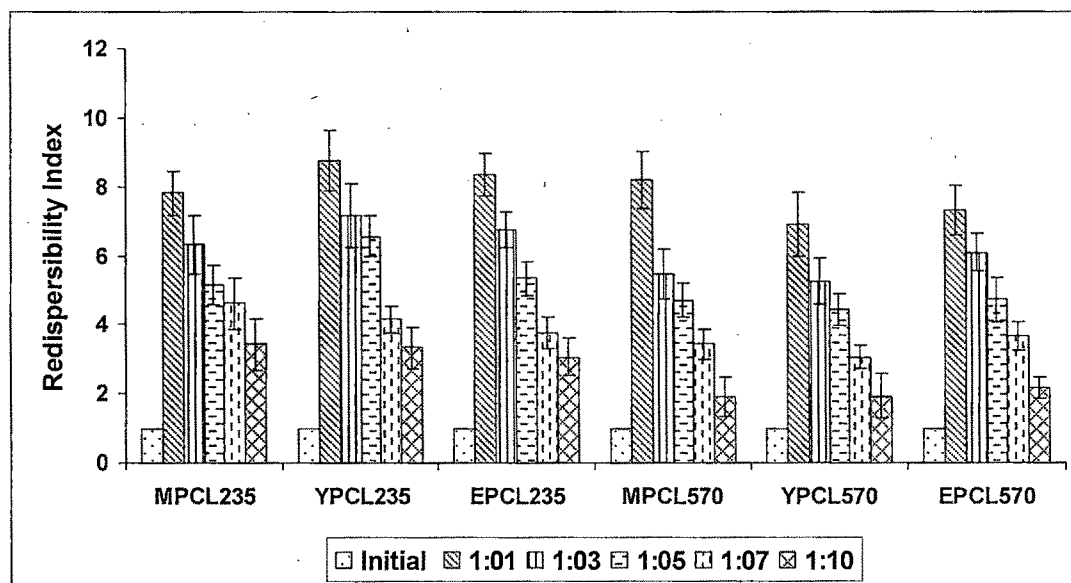


Figure 6.5 Redispersibility index of micellar formulations at various weight ratios of total solid content to sucrose (n=3)

Ratio*	Redispersibility index (RI) \pm S.D.					
	MPCL235	YPCL235	EPCL235	MPCL570	YPCL570	EPCL570
Initial Particle Size (nm)						
	38.45 \pm 4.61	44.01 \pm 3.09	47.01 \pm 2.28	73.31 \pm 3.70	86.21 \pm 4.18	80.10 \pm 4.77
1:1	24.81 \pm 1.82	23.17 \pm 2.29	20.72 \pm 2.57	18.07 \pm 2.63	16.53 \pm 2.60	15.09 \pm 3.01
1:3	23.32 \pm 1.29	21.52 \pm 1.81	19.32 \pm 1.77	13.75 \pm 0.82	13.56 \pm 0.76	13.22 \pm 1.20
1:5	19.67 \pm 1.10	17.63 \pm 1.38	15.52 \pm 1.41	3.99 \pm 0.46	3.68 \pm 0.56	4.19 \pm 0.91
1:7	12.39 \pm 0.99	13.36 \pm 0.84	9.96 \pm 0.62	5.60 \pm 0.58	5.19 \pm 0.78	4.38 \pm 0.75
1:10	11.94 \pm 1.01	13.42 \pm 0.79	10.43 \pm 0.66	5.48 \pm 0.80	5.26 \pm 0.51	5.01 \pm 0.66

* Weight ratio of total solid content to trehalose

Table 6.6 Redispersibility index of micellar formulations at various weight ratios of total solid content to trehalose (n=3)

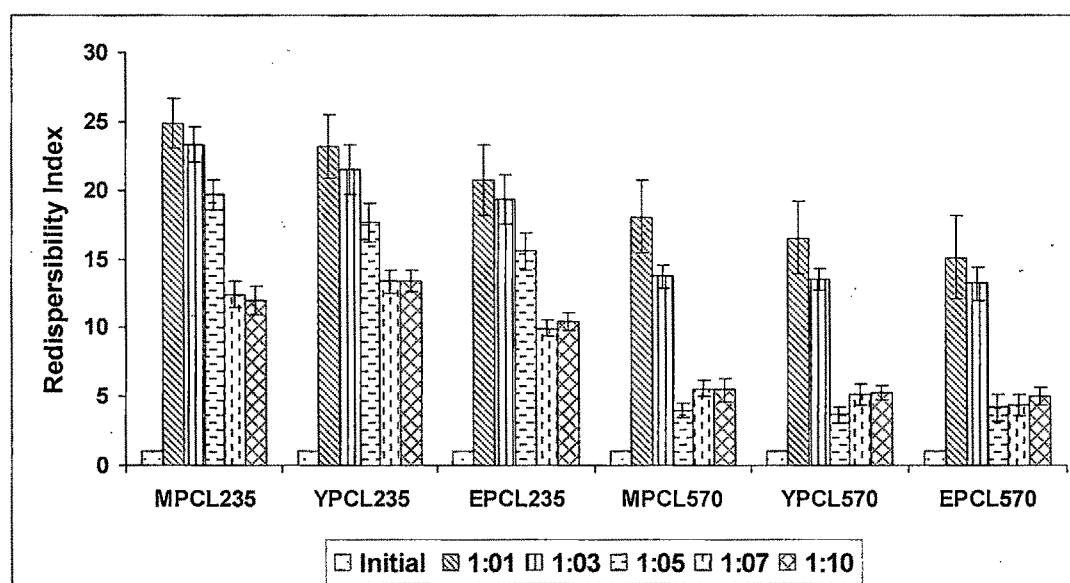


Figure 6.6 Redispersibility index of micellar formulations at various weight ratios of total solid content to trehalose (n=3)

As shown in Table 6.5 and 6.6, it was found that both sucrose and trehalose were unable to preserve the original particle size. Sucrose used at maximum ratio (1:10) of total solid content to sucrose showed redispersibility index from 1.9 to 3.4 (Table 6.5 & Figure 6.5). This implies that sucrose is not capable to preserve the original particle size upto ratio of 1:10. Trehalose which is considered as a best cryoprotectant for

nanocarrier during lyophilization gave unsatisfactory results and the redispersibility index obtained was very much high compared to sucrose. At 1:7 ratio of total solid content to trehalose, MPCL235, YPCL235 and EPCL235 showed redispersibility index between 10 to 14, while MPCL570, YPCL570 and EPCL570 at same ratio showed redispersibility index between 5 to 6 (Table 6.6 & Figure 6.6). Moreover, there was no significant difference in particle size was observed after reconstitution was observed 1:7 and 1:10 weight ratio which might be due to saturation of lyoprotective activity of trehalose (Jaeghere et al., 1999). A difference in redispersibility index between MPCL235, YPCL235 & EPCL235 to MPCL570, YPCL570 & EPCL570 at all ratio with use of sucrose and trehalose was also seen, which was assumed due to difference in PEG content as well as molecular weight in both the group of micelles. It was concluded that complete redispersion of micellar formulation was not feasible using sucrose and trehalose as cryoprotectant due to partial protection offered by them during freeze drying.

A complete redispersion with RI near to 1 was not achieved at different ratio of total solid content to trehalose, as reported by Jaeghere et al. (1999) in PLA-PEO nanoparticles. The probable reason behind this could be due to high PEG concentration, presence of drug and molecular weight of di-block copolymer used. The results obtained proved that trehalose is not a suitable candidate as cryoprotectant for micelles made of PEG and PCL blocks. PEG which is having inherent properties of steric stabilization in aqueous colloidal dispersion was unable to maintain the original particle size in absence of cryoprotectants (Jaeghere et al., 1999). The reason for this differential behavior has been attributed to the tendency of PEG to crystallize during freeze drying (Izutsu et al., 1996). In addition, due to covalent attachment of PEG to surface, an intra and inter particulate bridges of crystallized PEG might have been formed during freezing, resulting in to aggregated particles after water removal which was evidenced in X-ray diffraction study carried out for MPCL235 and MPCL570.

Layre et al. (2006) studied the effect of four sugars (glucose, saccharose, maltose, and trehalose) and one surfactant (Poloxamer-188), on freeze-drying of PIBCA and PCL-PEG nanoparticles. It was found that in absence of Poloxamer-188, a significant increase in particle size after freeze drying took place and all four sugars failed to

protect the nanoparticles against aggregation during freeze drying. In contrast to this, nanoparticles freeze dried in presence of poloxamer-188 showed tyndall effect upon redispersion and concluded that poloxamer-188 is required to maintain the original particle size after freeze drying. Based on above finding (Layre et al., 2006), poloxamer-188 was tried with sucrose at different ratio as shown in Table 6.7.

Ratio*	Redispersibility index (RI) ± S.D.					
	MPCL235	YPCL235	EPCL235	MPCL570	YPCL570	EPCL570
P. Size# (nm)	40.32 ± 3.07	45.90 ± 4.71	46.32 ± 3.13	72.01 ± 6.01	84.59 ± 5.21	85.11 ± 4.67
1:10:3	3.26 ± 0.16	3.21 ± 0.16	3.10 ± 0.16	2.67 ± 0.12	2.40 ± 0.13	2.53 ± 0.15
1:10:5	3.55 ± 0.23	3.65 ± 0.18	3.63 ± 0.23	3.17 ± 0.17	2.77 ± 0.16	2.75 ± 0.17
1:10:7	4.74 ± 0.20	4.69 ± 0.33	4.40 ± 0.19	3.75 ± 0.19	3.47 ± 0.28	3.29 ± 0.22
1:10:10	6.89 ± 0.54	6.95 ± 0.53	6.24 ± 0.52	4.89 ± 0.45	4.12 ± 0.35	4.34 ± 0.42
1:5:2	1.92 ± 0.17	1.57 ± 0.14	1.43 ± 0.14	1.14 ± 0.09	1.15 ± 0.05	1.19 ± 0.07
1:5:4	1.32 ± 0.12	1.56 ± 0.16	1.39 ± 0.11	1.39 ± 0.10	1.46 ± 0.09	1.49 ± 0.06
1:5:6	3.03 ± 0.15	2.75 ± 0.18	2.51 ± 0.13	2.00 ± 0.14	2.01 ± 0.11	2.15 ± 0.18

* Weight Ratio of total solid content: sucrose: poloxamer-188

Initial particle size (nm)

Table 6.7 Redispersibility index of micellar formulations using various ratio of total solid content to sucrose and poloxamer-188 (n=3)

Promising results were obtained with the use of surfactant poloxamer-188 along with sucrose (Table 6.7 & Figure 6.7). Although, when particle size was measured after reconstitution, it was observed that weight ratio still affected much on particle size. At 1:10:5 ratios, redispersibility index obtained was in between 2.75 to 3.65. MPCL235, YPCL235 and EPCL235 showed a minimum redispersibility index near to 1 at 1: 5: 4 ratio while MPCL570, YPCL570 and EPCL570 exhibited refractive index near to 1 at 1: 5: 2 ratios. A different ratio required for both groups to achieve redispersibility index near to one might be due to changes in PEG content in micelles.

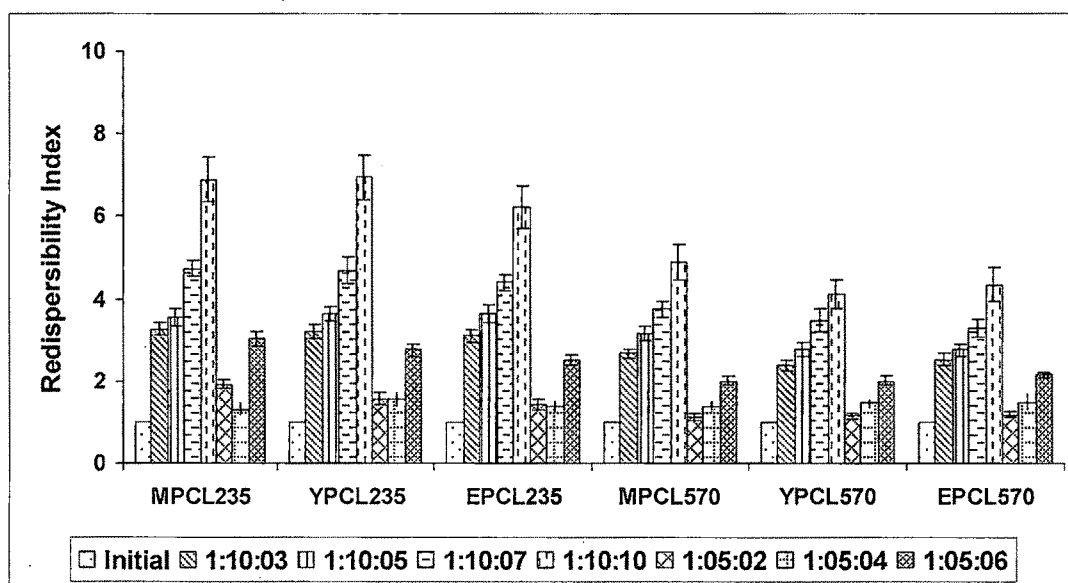


Figure 6.7 Redispersibility index of micellar formulations using various ratio of total solid content to sucrose and poloxamer-188 (n=3)

6.4.2.5 *In vitro* release studies

The release profile of drug from micelles is quite complex and can be affected by various factors like polymer degradation, molecular weight, crystallinity, glass transition temperature and binding affinity of drug to polymer (Shin et al., 1998). *In vitro* release studies of formulation were performed in phosphate buffer saline, pH 7.4 to correlate the predictable drug release *in vivo*. The percent cumulative release profile of MPCL235, YPCL235 and EPCL235 was depicted in Table 6.8 & Figure 6.8 and for MPCL570, YPCL570 and EPCL570 the release profile was represented in Table 6.9 and Figure 6.9. After 12 h, MPCL235, YPCL235 and EPCL235 showed drug release of 22.99 ± 4.76 , 16.34 ± 3.56 and 19.38 ± 4.44 percent respectively, while MPCL570, YPCL570 and EPCL570 at the same time exhibited drug release of 17.98 ± 3.98 , 9.08 ± 3.01 and 11.69 ± 4.40 percent respectively. The initial release upto 24 h was attributed to the presence of drug deposited on the surface or in the microchannels probably existing in micelles (Ge et al., 2002).

Time (h)	% Cumulative release		
	MPCL235	YPCL235	EPCL235
1	3.32 ± 1.12	2.45 ± 1.23	2.67 ± 1.28
3	9.56 ± 2.88	5.57 ± 2.65	5.51 ± 3.01
6	16.82 ± 3.09	10.76 ± 2.76	13.22 ± 3.10
12	22.99 ± 4.76	16.34 ± 3.56	19.38 ± 4.44
24	43.01 ± 4.90	32.11 ± 4.21	35.45 ± 5.02
48	63.18 ± 6.38	46.70 ± 4.76	48.84 ± 5.34
72	84.76 ± 6.67	59.08 ± 6.03	57.36 ± 7.27
96	89.05 ± 5.69	69.84 ± 4.90	72.38 ± 5.09
120	94.33 ± 5.28	76.34 ± 5.78	79.11 ± 5.47
144	95.80 ± 6.90	83.44 ± 5.44	85.24 ± 5.13

Table 6.8 *In vitro* release study profile of MPCL235, YPCL235 and EPCL235 micelles in PBS pH 7.4 (Results are mean ± S. D. of three individual experiments)

Time (h)	% Cumulative release		
	MPCL570	YPCL570	EPCL570
1	2.23 ± 1.13	0.22 ± 0.13	0.35 ± 0.22
3	5.50 ± 2.08	3.79 ± 2.05	4.07 ± 1.91
6	10.32 ± 3.19	7.06 ± 2.71	8.43 ± 3.47
12	17.98 ± 3.98	9.08 ± 3.01	11.69 ± 4.40
24	22.56 ± 4.88	16.31 ± 4.24	15.40 ± 5.31
48	38.90 ± 5.38	32.09 ± 4.86	30.43 ± 5.70
72	58.09 ± 4.67	40.10 ± 5.58	43.23 ± 4.33
96	67.43 ± 5.09	50.34 ± 7.09	50.23 ± 5.65
120	72.30 ± 5.90	56.23 ± 6.78	59.08 ± 4.41
144	74.32 ± 5.71	61.71 ± 6.94	63.33 ± 5.63

Table 6.9 *In vitro* release study profile of MPCL570, YPCL570 and EPCL570 micelles in PBS pH 7.4 (Results are mean ± S. D. of three individual experiments)

After 144 hr (6 day), MPCL235 micelles showed 95.80 ± 6.90 percent release while YPCL235 and EPCL235 showed 83.44 ± 5.44 & 85.24 ± 5.13 percent drug release respectively at the same time point. MPCL570 micelles exhibited 74.32 ± 5.71 percent drug release at 144 hr (6 day), while YPCL570 and EPCL570 showed 61.71 ± 6.94 & 63.33 ± 5.63 percent drug release respectively at same time point. This suggests that as time proceeds, the release profile of drug changes with respect to time and drug release was more dependent on molecular weight of PCL block (Kim et al., 1998). The drug release rate observed in the present study could not be mainly affected by polymer degradation as PCL degrades quite slowly during release process (Ge et al., 2002) and in this case, the release rate might be mainly affected by the diffusion of the drug through the polymer matrix.

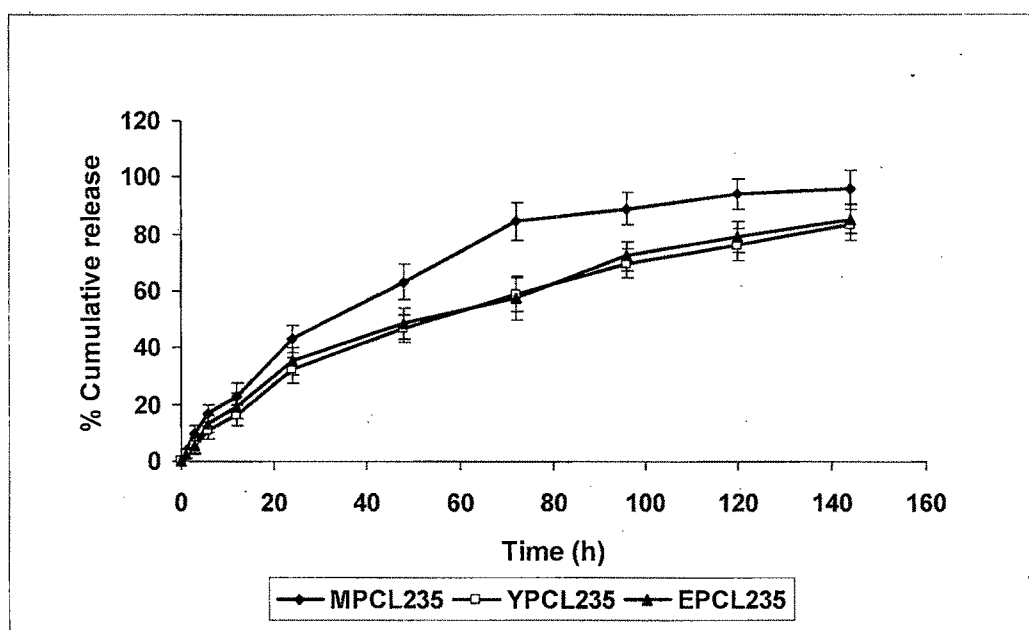


Figure 6.8 *In vitro* release study profile of MPCL235, YPCL235 and EPCL235 micelles in PBS pH 7.4

A significant difference in drug release profile was also observed between MPCL235 to YPCL235 and EPCL235, which was due to loss of drug adsorbed at the surface during peptide conjugation procedure. This phenomenon was also exhibited by YPCL570 and EPCL570 micelles compared to MPCL570.

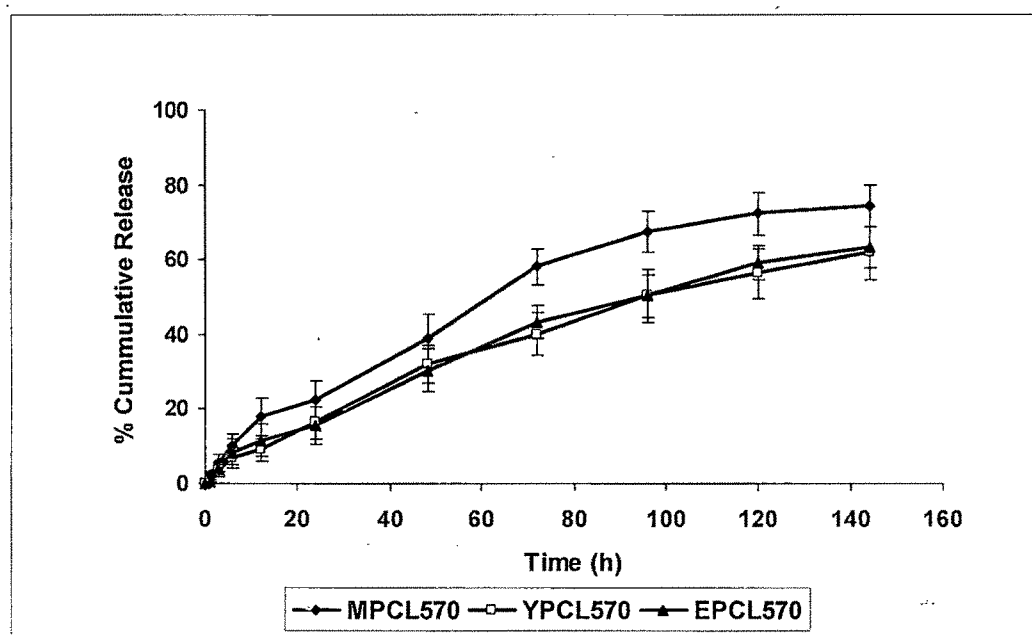


Figure 6.9 *In vitro* release study profile of MPCL570, YPCL570 and EPCL570 micelles in PBS pH 7.4

6.4.2.6 Stability studies

Stability is defined as the capacity of a drug substance or drug product to remain within established specifications to maintain its identity, strength, quality and purity throughout the retest or expiration dating periods (Draft guidance, Stability Testing of Drug Substances and Drug Products, FDA, 1998). Stability testing provides evidence that the quality of drug substance or drug product under the influence of various environmental factors changes with time (ICH Draft guidance, Stability Testing of New Drug Substance and Products, QIA (R2), 2003). In order to improve the physical and chemical stability of micellar or nanoparticles water has to be removed by a process called freeze drying. A short term stability studies were performed at two different conditions i.e. at $2-8^{\circ}\text{C}$ and at $25 \pm 2^{\circ}\text{C}$ with $60 \pm 5\%$ RH to find out the effect of storage conditions on particle size and percent drug loading.

Formulation code	Initial*	2-8 °C			25 ± 2 °C with 60 ± 5 % RH.		
		1 month	2 month	3 month	1 month	2 month	3 month
MPCL235	52.72 ± 5.09	53.30 ± 7.23	56.90 ± 6.09	58.73 ± 7.31	55.95 ± 5.23	60.14 ± 7.33	70.89 ± 7.02
YPCL235	68.83 ± 6.88	69.63 ± 8.45	74.34 ± 7.45	76.25 ± 5.67	72.22 ± 9.02	78.35 ± 6.68	85.73 ± 8.66
EPCL235	65.77 ± 5.30	68.25 ± 5.78	74.72 ± 8.39	76.26 ± 5.34	68.12 ± 6.76	75.55 ± 9.02	86.95 ± 7.70

* Particle size measured after reconstitution of lyophilized product.

Table 6.10 Influence on particle size of MPCL235, YPCL235 and EPCL235 micelles at different storage conditions (Results are mean ± S. D. of three experiments)

Formulation code	Initial	2-8 °C			25 ± 2 °C with 60 ± 5 % RH.		
		1 month	2 month	3 month	1 month	2 month	3 month
MPCL235	3.89 ± 0.17	3.88 ± 0.10	3.87 ± 0.19	3.88 ± 0.21	3.89 ± 0.11	3.88 ± 0.20	3.87 ± 0.19
YPCL235	3.38 ± 0.12	3.37 ± 0.16	3.37 ± 0.15	3.36 ± 0.17	3.37 ± 0.14	3.36 ± 0.22	3.35 ± 0.13
EPCL235	3.27 ± 0.21	3.28 ± 0.13	3.27 ± 0.17	3.26 ± 0.08	3.27 ± 0.23	3.26 ± 0.13	3.25 ± 0.11

Table 6.11 Influence on percent drug loading of MPCL235, YPCL235 and EPCL235 micelles at different storage conditions (Results are mean ± S. D. of three experiments)

Formulation code	Initial*	2-8 °C			25 ± 2 °C with 60 ± 5 % RH.		
		1 month	2 month	3 month	1 month	2 month	3 month
MPCL570	82.23 ± 6.80	84.53 ± 5.01	87.98 ± 8.15	90.43 ± 7.34	89.65 ± 6.20	92.21 ± 8.80	98.53 ± 8.31
YPCL570	96.80 ± 4.89	97.65 ± 6.28	101.4 ± 7.01	103.3 ± 8.95	102.3 ± 6.02	110.2 ± 7.96	116.2 ± 9.24
EPCL570	98.15 ± 5.87	100.3 ± 4.92	101.8 ± 6.33	107.2 ± 6.06	100.3 ± 5.31	109.4 ± 6.99	120.6 ± 8.62

* Particle size measured after reconstitution of lyophilized product.

Table 6.12 Influence on particle size of MPCL570, YPCL570 and EPCL570 micelles at different storage conditions (Results are mean ± S. D. of three experiments)

Formulation code	Initial	2-8 °C			25 ± 2 °C with 60 ± 5 % RH.		
		1 month	2 month	3 month	1 month	2 month	3 month
MPCL570	4.36 ± 0.13	4.35 ± 0.21	4.35 ± 0.20	4.34 ± 0.25	4.36 ± 0.25	4.34 ± 0.21	4.33 ± 0.23
YPCL570	3.71 ± 0.18	3.71 ± 0.18	3.70 ± 0.21	3.70 ± 0.22	3.70 ± 0.18	3.69 ± 0.26	3.69 ± 0.16
EPCL570	3.65 ± 0.15	3.64 ± 0.17	3.64 ± 0.13	3.63 ± 0.20	3.64 ± 0.18	3.63 ± 0.17	3.63 ± 0.15

Table 6.13 Influence on percent drug loading of MPCL570, YPCL570 and EPCL570 micelles at different storage conditions (Results are mean ± S. D. of three experiments)

The stability study results obtained are depicted in Table 6.10 to 6.13. It was noticed that a negligible increase in particle size (upto 10 percent) was found in MPCL235, YPCL235 and EPCL235 micellar formulation when stored at 2-8 °C after three month of storage compared to 25 ± 2 °C with 60 ± 5 % RH storage condition which resulted in to rise in particle size upto 32 percent (Table 6.10). Moreover, there was no any change in percent drug loading observed at both the storage conditions (Table 6.11).

Similarly, in case of MPCL570, YPCL570 and EPCL570 particle size increased upto 9 percent when stored at 2-8 °C after three months (Table 6.12), while storage at 25 ± 2 °C with 60 ± 5 % RH, particle size increased upto 23 percent. No significant change in percent drug loading was observed at both the storage conditions as shown in Table 6.13. It was concluded that the micellar formulation would be stable at 2-8 °C for longer period of time without much influence on particle size and percent drug loading.

REFERENCES

Abdelwahed W, Degobert G, Stainmesse S, Fessi H. Freeze-drying of nanoparticles: Formulation, process and storage considerations. *Adv Drug Deliv Rev* 2006; 58: 1688–1713.

Allison SD, Dong A, Carpenter JF. Counteracting effects of thiocyanate and sucrose on chymotrypsinogen secondary structure and aggregation during freezing, drying, and rehydration. *Biophys J* 1996; 71:2022-2032.

Allison SD, Randolph TW, Manning MC, Middleton K, Davis A, Carpenter JF. Effects of drying methods and additives on structure and function of actin: mechanisms of dehydration induced damage and its inhibition. *Arch Biochem Biophys* 1998; 358: 171-181.

Atyabi F, Farkhondehfar A, Esmacily F, Dinarvand R. Preparation of pegylated nano-liposomal formulation containing SN-38: in vitro characterization and in vivo biodistribution in mice. *Acta Pharm* 2009; 59: 133-144.

Auvillain M, Cave G, Fessi H, Devissaguet JP. Lyophilisation de vecteurs colloïdaux submicroniques. *STP Pharma* 1989; 5: 738-744.

Chacon M, Molpeceres J, Berges L, Guzman M, Aberturas MR. Stability and freeze-drying of cyclosporine loaded poly(D,L lactide-glycolide) carriers. *Eur J Pharm Sci* 1999; 8: 99-107.

Farokhzad OC, Sangyong J, Ali K, Thanh-Nga TT, David AL, Robert L. Nanoparticle-aptamer bioconjugates: A new approach for targeting prostate cancer cells. *Cancer Res* 2004; 64: 7668-7672.

Forrest ML, Zhao A, Won CY, Malick AW, Kwon GS. Lipophilic prodrugs of Hsp90 inhibitor geldanamycin for nanoencapsulation in poly(ethylene glycol)-b-poly(ϵ -caprolactone) micelles. *J Control Release* 2006a; 116: 139-149.

Forrest ML, Won CY, Malick AW, Kwon GS. In vitro release of the mTOR inhibitor rapamycin from poly(ethylene glycol)-b-poly(ϵ -caprolactone) micelles. *J Control Release* 2006b; 110: 370- 377.

Ge H, Hu Y, Jiang X, Cheng D, Yuyan Y, Bi H, Yang C. Preparation, characterization, and drug release behaviors of drug nimodipine-loaded poly(ϵ -caprolactone)-poly(ethylene oxide)-poly(ϵ -caprolactone) amphiphilic triblock copolymer micelles. *J Pharm Sci* 2002; 91: 1463-1473.

Grabarek Z, Gergely J. Zero-length crosslinking procedure with the use of active esters. *Anal Biochem* 1990; 185:131-135.

Gu F, Zhang L, Teply BA, Nina Mann N, Wang A, Radovic-Moreno AF, Langer R, Farokhzad OC. Precise engineering of targeted nanoparticles by using self-assembled biointegrated block copolymers. *Proc Natl Acad Sci USA* 2008; 105: 2586-2591.

Izutsu KI, Yoshioka S, Kojima S, Randolph TW, Carpenter JF. Effects of sugar and polymers on crystallization of poly(ethylene glycol) in frozen solutions: phase separation between incompatible polymers. *Pharm Res* 1996; 13: 1393-1400.

Jaeghere D, Allemann F, Leroux E, Stevels JC, Feijen W, Doelker J, Gurny R. Formulation and lyoprotection of poly(lactic acid-co-ethylene oxide) nanoparticles: influence on physical stability and in vitro cell uptake. *Pharm Res* 1999; 16: 859-866.

Jasti BR, Du J, Vasavada RC. Characterization of thermal behavior of etoposide. *Int J Pharm* 1995; 118: 161-167.

Kim SY, Shin IG, Lee YM, Cho CS, Sung YK. Methoxy poly(ethylene glycol) and epsilon-caprolactone amphiphilic block copolymeric micelle containing indomethacin. II. Micelle formation and drug release behaviours. *J Control Release* 1998; 51: 13-22

Layre AM, Couvreur P, Richard J, Requier D, Eddine G, Gref R. Freeze-drying of composite core-shell nanoparticles. *Drug Dev Ind Pharm* 2006; 32: 839-846.

Leamon CP, Low PS. Delivery of macromolecules into living cells: a method that exploits folate receptor endocytosis. *Proc Natl Acad Sci USA* 1991; 88: 5572-5576.

Lee RJ, Low PS. Delivery of liposomes into cultured KB cells via folate receptor-mediated endocytosis. *J Biol Chem* 1994; 269: 3198-3204.

Lin WJ, Wang CL, Chen YC. Comparison of two pegylated copolymeric micelles and their potential as drug carriers. *Drug Deliv* 2005; 12: 223-227.

Lopez BA, Polo D, Reig Z, Fabra A. Pentapeptide YIGSR-mediated HT-1080 fibrosarcoma cells targeting of adriamycin encapsulated in sterically stabilized liposomes. *J Biomed Mater Res* 2004; 69A: 155-163.

Saez A, Guzman M, Molpeceres J, Aberturas MR. Freeze drying of polycaprolactone and poly (D,L-lactic-glycolic) nanoparticles induce minor particle size changes affecting the oral pharmacokinetics of loaded drugs. *Eur J Pharm Biopharm* 2000; 50: 379-387.

Shin IG, Kim SY, Lee YM, Cho CS, Sung YK. Methoxy poly(ethylene glycol)/ε-caprolactone amphiphilic block copolymeric micelle containing indomethacin. I. preparation and characterization. *J Control Release* 1998; 51: 1-11.

Snehalatha M, Venugopal K, Saha RN. Etoposide-loaded PLGA and PCL nanoparticles I: preparation and effect of formulation variables. *Drug Deliv* 2008; 15: 267-275.

Staros JV, Wright RW, Swingle DM. Enhancement by N-hydroxysulfosuccinimide of water-soluble carbodiimide mediated coupling reactions. *Anal Biochem* 1986; 156: 220-222.

Sutton D, Nasongkla N, Blanco E, Gao J. Functionalized micellar systems for cancer targeted drug delivery. *Pharm Res* 2007; 24: 1029-1046.

Yang Z, Liu J, Huang Z, Shi W. Crystallization behavior and micelle formation of star-shaped amphiphilic block copolymer based on dendritic poly(ether-amide). *Eur Pol J* 2007; 43: 2298-2307.

Zhang L, Hu Y, Jiang X, Yang C, Lu W, Yang YH. Camptothecin derivative-loaded poly(caprolactone-co-lactide)-b-PEG-b-poly(caprolactone-co-lactide) nanoparticles and their biodistribution in mice. *J Control Release* 2004; 96: 135-148.

Zhang X, Jackson JK, Burt HM. Development of amphiphilic diblock copolymers as micellar carriers of taxol. *Int J Pharm* 1996; 132: 195-206.

Zhao H, Yung LY. Selectivity of folate conjugated polymer micelles against different tumor cells. *Int J Pharm* 2008; 349: 256-268.